1 **Simultaneous recovery of ammonium and phosphate from simulated treated wastewater**

2 **effluents by activated calcium and magnesium zeolites**

3

4 Xialei You[a]*, César Valderrama[a] and José Luis Cortina[a,b]

5 [a] Department of Chemical Engineering. Universitat Politècnica de Catalunya-Barcelona-TECH

6 (UPC), Spain

7 [b] Water Technology Center, CETaqua, Carretera d'Esplugues 75, Cornellá de Llobregat, 08940

8 Spain

9

10 *Correspondence should be addressed to: Xialei You

11 Departament of Chemical Engineering, Universitat Politècnica de Catalunya-Barcelona Tech

12 (UPC)

13 Avda. Diagonal, 647 (08028) Barcelona, Spain

14 Tel.: 93 401 66 45

15 Email: xialei.you@upc.edu

16

17 **Abstract**

18 BACKGROUND: In this study a sodium zeolite synthesized from coal fly ash (NaP1-NA) was

19 modified to calcium and magnesium forms (Ze-Ca, Ze-Mg) as sorbent materials for simultaneous

20 recovery of ammonium and phosphate from simulated treated wastewaters effluents.

21 RESULTS: Increasing the temperature during the modification step to magnesium form improved

22 the zeolite conversion. The maximum sorption capacities obtained were 123.1±9.1 mg NH_4/g and

23 119.5±7.5 mg PO_4/g in ammonium/phosphate binary system for Ze-Ca, while 55.2±2.4/ 60.5

24 ±14.1 and 32.3±4.4/ 23.9±3.4 were obtained for Ze-Mg1 and Ze-Mg2, respectively. The sorption

1

1   process is faster for Ze-Mg zeolites and the sorption mechanism that controls the overall process,

2   for both zeolites, is the diffusion into the particle according to the HPDM and SPM models.

3   CONCLUSIONS: Salt modification improved the performance of zeolites towards phosphate

4   sorption. The sorption mechanism involves both: ammonium exchange to the Mg and Ca ions,

5   and precipitation of Ca and Mg phosphates or mixed ammonium-magnesium phosphate minerals

6   such as brushite ($CaHPO_4.H_2O$) and struvite ($MgNH_4PO_4$).

7

8   **Keywords:** Zeolites; ion exchange; precipitation; waste-water

9

10 **1. Introduction**

11 Nitrogen and phosphorus, mainly in the form of ammonium and phosphate, are the two most

12 prominent macronutrients in aquatic systems. They can act as limiting nutrients but the

13 overloading of dissolved nutrients in aquatic systems can result in eutrophication, reporting a

14 severe reduction in aquatic life diversity and quality. It is worth to point out that many estuarine

15 and freshwater systems tend toward phosphorus limitation while marine systems tend towards

16 nitrogen limitation [1].

17 Human manipulation of nitrogen and phosphorus cycle is intense as large amounts of these

18 elements are needed for fertilizer production in order to supply growing population food demand

19 [2]. Alteration of these natural cycles leads to problems with air and water quality as well as

20 ecosystem integrity [3–6]. Thus, in the last years, several studies have been focused on the removal

21 but also in the recovery of these nutrients in order to close the anthropogenic cycle of nitrogen

22 and phosphorus. In order to achieve this goal, several studies have been carried out for

23 recovering these nutrients from wastewater treatment plants (WWTPA) effluents, mainly by

24 adsorption and precipitation process.

1   Zeolites are a promising option to be used as low-cost sorbent material for wastewater treatment

2   [7]. Moreover, they have been widely studied for nutrients removal and recovery from wastewater

3   as they report high internal porosity which allows water retention, a uniform particle size

4   distribution and high cation-exchange capacity for nutrients retaining, specially ammonium ions

5   [8,9].

6   Ammonium sorption onto zeolites is carried out mainly by ion exchange and the sorption capacity

7   increases with the increase of the Siliceous Aluminum Ratio (SAR) [10]. Phosphate sorption onto

8   zeolites occurs rarely and mainly by the complexation with AlOH and FeOH present in zeolite

9   structure. Therefore, to improve phosphate sorption performance as well as to provide higher

10   selectivity towards oxyanions sorption was studied the incorporation of divalent or trivalent

11   metallic ions such as Ca^{2+}, Mg^{2+}, Fe^{3+} and La^{3+} through ion exchange in a salt modification

12   pretreatment of zeolites. Most of cases that pretreatment was carried out at high temperature in

13   order to favor the ion exchange as zeolites present more affinity towards monovalent ions [11–16].

14   In addition, applications of zeolites in agriculture are being investigated, especially as a carrier for

15   slow release fertilizers [17] as they reported the availability for improving soil physico-chemical and

16   microbial capacity [18] and enhancing nitrogen and phosphorus use efficiently [19–21]. For this

17   purpose, simultaneous recovery of ammonium and phosphate by zeolites may represent many

18   advantages as loaded zeolites could be used as slow release fertilizer. Although there are many

19   studies for simultaneous removal of these nutrients by using polymeric sorbents and biochar [22,23]

20   or biological treatment [24,25], there is lack of research for simultaneous recovery of ammonium and

21   phosphate by using zeolites [11,15,26]. Sodium zeolites with intrinsic properties for ammonium

22   removal could be modified to the magnesium and calcium forms to promote the removal of

23   phosphate by formation of calcium- or magnesium-phosphates.

24   This study describes the performance of three modified synthetic zeolites, to calcium and

25   magnesium form, for simultaneous removal and recovery of ammonium and phosphate from

1   synthetic solutions simulating wastewater treatment effluents. The effect of temperature on zeolite

2   modification process and consequently on sorption mechanism was studied by using two

3   modification methods for zeolites in magnesium form. Furthermore, equilibrium studies were

4   performed by isotherms test in ammonium single and ammonium/phosphate binary experiments.

5   Finally, the nutrients uptake rate-limiting step was evaluated by fitting kinetic experimental data to

6   the Homogeneous Particle Diffusion Model (HPDM), the Shell Progressive Model (SPD) and the

7   Intraparticle Diffusion Model.

8

9   **2. Materials and methods**

10   **2.1. Preparation of Calcium and Magnesium modified zeolites**

11   A sodium zeolite (Ze-Na) was synthesized from coal fly ash by using a 3 M NaOH solution at 125

12   ºC and 8 h of reaction [27,28]. Then, this zeolite in sodium form was used to prepare Ca and Mg

13   forms (Ze-Ca, ZeMg). The conversion procedure was adapted from the method reported by Wu

14   et al. [15].

15   A pretreatment step was carried out as follows; 30 g of Ze-Na was placed in a flask and was

16   mixed with 250 mL of 1 M NaCl solution. The slurry was boiled with reflux for 4 h with continuous

17   stirring. The solid phase was separated by filtration and was mixed with 250 mL of 1 M CaCl$_2$ or

18   MgCl$_2$ solution and the slurry stirred continuously at two different temperatures: i) at 100 ºC and ii)

19   at room temperature. As the sodium/magnesium exchange is not favored at room temperatures

20   the influence of the temperature on zeolite modification was studied using two types of zeolites,

21   Ze-Mg1 (at 100 ºC) and Ze-Mg2 (at 25 °C). The solid phases (Ze-Ca, Ze-Mg1 and Ze-Mg2) were

22   separated by filtration and washed with deionized water for several times in order to wash out

23   residual salts and then were dried in an oven at 50 ºC for 72 h and stored in airtight containers for

24   subsequent experiments.

25

1 **2.2. Sorption equilibrium experiments: single and binary systems**

2 The prepared testing samples pretends to simulate the secondary effluent from WWTP, the main

3 characteristics of the effluent are: TSS [mg/L]: 44; NH_4^+ [mg NH_4/L]: 1.0; Total P [mg P/L]: 12;

4 PO_4^{3-} [mg PO_4/L]: 7.2; Alkalinity [mg $CaCO_3$/L]: 400; Ca [mg/L]: 212; Mg [mg/L]: 68; K [mg/L]: 36;

5 SO_4^{2-} [mg SO_4/L]: 124; Cl^- [mg Cl/L]: 326; pH: 7.4 The composition was slightly modified in order

6 to obtain a proper ammonium - phosphate ratio for struvite precipitation.

7 Equilibrium sorption experiments were carried out by using standard methodology described in

8 previous works [29]. For ammonium single experiments, 25 mL of ammonium test solution (5–5000

9 mg L^{-1}) were mixed mechanically with 0.1 g of zeolites until equilibrium was achieved (24 h). For

10 binary systems (ammonium/phosphate), the procedure was repeated with test solutions

11 containing ammonium in the concentration range of 2-4000 mg L^{-1} and phosphate in the

12 concentration range of 6-12000 mg L^{-1}. After phase separation, total ammonium and phosphate

13 concentration were determined appropriately. Standard methods were used for phosphate and

14 ammonium quantification. The phosphate concentration was analyzed by the

15 vanadomolybdophosphoric acid colorimetric method (4500-P C) and ammonium was determined

16 by ammonia-selective electrode method (4500-NH3 D). Thermo Scientific Ionic Chromatograph

17 (Dionex ICS-1100 and ICS-1000) was used for ions determination. Tests were performed by

18 duplicate at 21±1 °C and average data are reported

19

20 **2.3. Sorption kinetic experiments: single and binary systems**

21 For kinetic studies, 1 g of zeolite was added into a glass flask containing 250 mL of a 10 mg L^{-1} of

22 ammonium solution. The system was agitated appropriately in order to maintain the sorbent

23 suspended in the solution. For binary samples a solution containing 5 mg L^{-1} of ammonium and

24 15 mg L^{-1} of phosphate were used. Samples of 6 mL were withdrawn at given times and total

1 ammonium and phosphate concentrations were determined. Tests were performed by duplicate

2 at 21 ± 1 °C and average data are reported.

3

4 **2.4. Physico-chemical characterization of zeolites**

5 Virgin Ze-Ca, Ze-Mg1 and Ze-Mg2 as well as loaded zeolites were washed with ultrapure water

6 and then were dried in the oven at 60 ºC for 24 h for physicochemical characterization.

7 Samples morphology as well as their chemical composition were analyzed by using a JEOL 3400

8 Field Emission Scanning Electron Microscope coupled to an Energy Dispersive Spectroscopy

9 system (FSEM-EDS). Reported samples composition is the average of three analyses in different

10 point of the sample.

11 The mineralogical composition was also analyzed by using a Bruker D8 A25 Advance X-Ray

12 Diffractometter. The specific surface area of samples was determined by the nitrogen gas

13 sorption method with an automatic sorption analyzer (Micrometrics). Infrared absorption spectra

14 in the range from 4000 to 550 cm^{-1} were obtained using a Fourier Transform FTIR 4100 Jasco

15 spectrometer. Particle size distribution of the zeolites were analyzed by laser light scattering (LS)

16 with a Coulter diffract particle size analyzer (LS 13 320 laser diffraction particle size analyzer

17 instrument, Beckman Coulter). The size crystal distribution range (CSD) detected was from 0.04

18 to 2000 μ m. The particle size expressed as both volume and number distributions allows one to

19 detect the presence of aggregates and to assess the size of the majority of the particles,

20 respectively. Particles were analyzed as the used for the batch experiments without any further

21 thermal treatment or/and granulometric separation

22

23 **2.5 Sorption equilibrium data treatment.**

24 The ammonium and phosphate equilibrium sorption data were fitted to the Langmuir (Eq. 1),

25 Freundlich (Eq. 2) and Langmuir-Freundlich (Eq. 3) isotherm equations through non-linear

6

1 regression by minimizing the Average Relative Error (Eq. 5) obtained as the average of

2 calculated Relative Errors between experimental and theoretical data (Eq. 4).

$$q = \frac{K_L q_m C_e}{1 + K_L C_e}$$ Eq. 1

$$q = K C_e^{\frac{1}{n}}$$ Eq. 2

$$q = \frac{q_m (K_{LF} C_e)^n}{(K_{LF} C_e)^n + 1}$$ Eq. 3

$$RE \, (\%) = \frac{|q_{exp} - q_{model}|}{q_{exp}} x100$$ Eq. 4

$$ARE \, (\%) = \frac{\sum_{i=1}^{n} RE_n}{n}$$ Eq. 5

3 where, q_m is the maximum loading of the sorbent (mg sorbate/g zeolite), K_L is the Langmuir

4 sorption constant (L/mg), K is the Freundlich sorption constant (mg/g)(mg/ L)$^{-1/n}$, n is the

5 Freundlich exponent and K_{LF} is the Langmuir-Freundlich sorption constant (L/mg).

6

7 **2.6 Sorption Kinetic data treatment.**

8 The rate limiting step of the sorption process can be determined using the Homogeneous Particle

9 Diffusion Model (HPDM) and Shell Progressive Model (SPM), widely used for fitting ion exchange

10 kinetics data [30,31]. The description and assumptions of both models can be consulted elsewhere

11 [32]. The rate controlling mechanism can be described by particle diffusion or liquid film diffusion in

12 the case of HPDM (Eq. 6 and 7) and fluid film control, particle control and chemical reaction

13 control for SPM (Eq.8-10).

$$-\ln\left(1 - \left(\frac{q_t}{q_e}\right)^2 (t)\right) = \frac{2\pi^2 D_e}{r^2} t$$ Eq. 6

$$-\ln\left(1 - \frac{q_t}{q_e}\right) = \frac{3DC}{rC_r} t$$ Eq. 7

7

1   where q_t and q_e are the sorbent capacity at time t and in equilibrium (mg·g^{-1}), D_e the effective

2   diffusion coefficient of sorbates in the zeolite (m^2·s^{-1}), r the radius of the zeolite particle (m), D

3   diffusion coefficient in solution (m^2·s^{-1}), C total concentration of adsorbing species (mol·dm^{-3}) and

4   C_r total concentration of adsorbing species in the zeolite (mol·dm^{-3}).

5

$$\frac{q_t}{q_e} = \frac{3C_{A0}K_F}{a_s r C_{S0}} t \qquad\qquad \text{Eq. 8}$$

$$3 - 3\left(1 - \frac{q_t}{q_e}\right)^{2/3} - 2X = \frac{6D_e C_{A0}}{a_s r^2 C_{S0}} t \qquad \text{Eq. 9}$$

$$1 - \left(1 - \frac{q_t}{q_e}\right)^{1/3} = \frac{k_s C_{A0}}{r} t \qquad\qquad \text{Eq.10}$$

6

7   where C_{A0} and C_{S0} are the concentration of adsorbing species A in bulk solution and at zeolite

8   particle unreacted core (mol·dm^{-3}), K_F the mass transfer coefficient of species A through the liquid

9   film (m·s^{-1}), a_s the stoichiometric coefficient, r the radius of the zeolite particle (m), D_e the effective

10   diffusion coefficient of sorbates in the adsorbent (m^2·s^{-1}) and k_s the reaction constant (m^2·s^{-1}).

11

12   **3. Results and discussion**

13   **3.1. Characterization of Ca and Mg modified zeolites**

14   The specific surface area of Ze-Na is significantly increased after salt modification from 6.3±0.8

15   to 17.0±1.1 m^2/g, 31.7±1.3 m^2/g and 16.4±1.1 m^2/g for Ze-Ca, Ze-Mg1 and Ze-Mg2, respectively.

16   The improvement of specific surface can be related to the pretreatment with sodium chloride as

17   well as to the heating treatment [33]. Moreover, SEM images showed a surface morphology with

18   homogeneous crystal size distribution for all zeolite samples indicating that salt modification

19   process does not represent significant morphological changes.

20   The FSEM-EDS analyses reported O, Na, Mg, Al, Si, Ca and Fe as the main elements on the Ze-

21   Na composition (Table 1). In Ze-Ca, the calcium content increased from 1.6% to 9.4%, whereas

8

1 magnesium content increased from 0.8% to 4.3% and 1.8% for Ze-Mg1 and Ze-Mg2,

2 respectively. In all cases, a significant decrease of sodium content was observed due to the ion

3 exchange process between sodium and calcium and magnesium ions.

4 **Table 1**

5 The FTIR spectra for Ze-Ca and Ze-Mg (Figure 1) reported peaks around 670 cm^{-1} and 970 cm^{-1}

6 attributed to the symmetric and the asymmetric internal stretching vibration of Si-O and Al-O

7 bounds in the tetrahedral structure, respectively.[34] The peak located in 1640 cm^{-1} is associated

8 with deformation vibration of water molecules due to the incomplete dehydration of zeolites.[14] It is

9 worth to mention that loaded Ze-Mg1 zeolite revealed two new peaks in comparison to raw

10 zeolite. These bands are characteristic of NH_4^+ (1434 cm^{-1}) and PO_4^{3-} (997 cm^{-1})[35,36], which is

11 similar to the bands showed by struvite according to RRUFF Spectrum Database for Struvite.

12

13 **Figure 1**

14 The X-Ray Diffraction patterns of Ze-Ca and both Ze-Mg zeolites identified mullite ($Al_6Si_2O_{13}$),

15 quartz (SiO_2) and garronite ($Ca_{2.8}(Al_{5.66}Si_{10.34}O_{32})(H_2O)_{13.76}$) as predominant phases. Particle size

16 analysis of both the Ze-Na and its modified forms (Ze-Ca/Ze-Mg) reported similar particle size

17 distribution. This indicates that the ion exchange process did not affect zeolitic structure. Particle

18 size analysis in volume of particles revealed the presence of zeolite particles with an average

19 equivalent diameter 29±1 μm for both Na and modified Ca/Mg samples. Analysis of samples

20 collected after the sorption experiments shown similar mean particle size (d_{50} value 27±2 μm).

21

22 **3.2. Ammonium and phosphate sorption capacity**

23 The experimental and the predicted equilibrium data based on isotherm models are shown in

24 Figure 2. The sorption parameters obtained by non-linear regression as well as ARE are

25 summarized in Table 2.
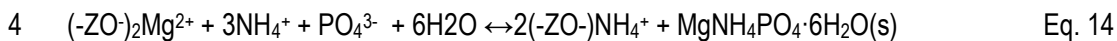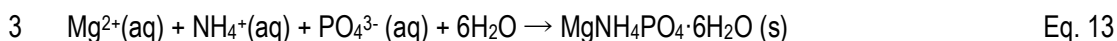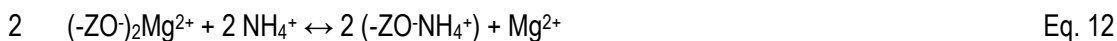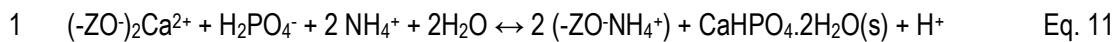
26 **Figure 2**

9

Table 2

Ammonium and phosphate extraction dependence on pH in the typical expected pH range of treated domestic wastewater effluents (e.g. 6 to 8.5) is very limited[11]. Values of pH below 3 ammonium sorption capacity is affected by the competition with H^+ and values above 10, sorption is diminished due to the conversion of NH_4^+ onto NH_3, that could not be extracted by the ionogenic groups of the zeolite.

Ammonium sorption data were well described by the Langmuir-Freundlich isotherm in all cases according to ARE values (See Supplementary Material Fig. S1). The results indicate that at low concentration levels, sorption follows Freundlich isotherm while at high concentration levels Langmuir isotherm equation fits better the experimental data. Thus, the sorption of ammonium onto zeolite combines mono-layered homogeneous and multilayered heterogeneous sorption mechanisms in both single and binary systems.

As can be seen in Figure 3, in the case of phosphate, sorption data were also well described by the Langmuir-Freundlich isotherm in all cases but ARE analysis showed that the Langmuir isotherm equation reported better fitting than Freundlich isotherm, which indicates that phosphate sorption onto zeolite can be assimilated to mono-layered homogeneous sorption.

Figure 3

The simultaneous removal of ammonium and phosphate by zeolites can be postulated by two different mechanisms: ion exchange and formation of calcium phosphate minerals in the case of Ze-Ca (Eq. 11) and struvite precipitation in the case of Ze-Mg1 and Ze-Mg2. It is important to point out that in the case of Ze-Mg1 the struvite precipitation is carried out both on zeolite surface and aqueous solution (Eq. 12-14) whereas in the case of Ze-Mg2, struvite formation is performed in the aqueous solution by the combination of released magnesium ions and ammonium and phosphate ions present in the aqueous solution. As a simple approach the ammonium and phosphate removal processes could be explained by the following reactions:[36]:

10

1 $(-ZO^-)_2Ca^{2+} + H_2PO_4^- + 2 NH_4^+ + 2H_2O \leftrightarrow 2 (-ZO \cdot NH_4^+) + CaHPO_4.2H_2O(s) + H^+$ Eq. 11

2 $(-ZO^-)_2Mg^{2+} + 2 NH_4^+ \leftrightarrow 2 (-ZO \cdot NH_4^+) + Mg^{2+}$ Eq. 12

3 $Mg^{2+}(aq) + NH_4^+(aq) + PO_4^{3-} (aq) + 6H_2O \rightarrow MgNH_4PO_4 \cdot 6H_2O (s)$ Eq. 13

4 $(-ZO^-)_2Mg^{2+} + 3NH_4^+ + PO_4^{3-} + 6H2O \leftrightarrow 2(-ZO-)NH_4^+ + MgNH_4PO_4 \cdot 6H_2O(s)$ Eq. 14

5 where $-ZO^-$ represents the anionic group on the zeolite structure.

6

7 Characterization of loaded zeolites showed the formation of brushite ($CaHPO_4.H_2O$) for Ze-Ca

8 and moreover the postulated sorption mechanism was confirmed by XRD (Figure 4). In the case

9 of Ze-Mg1, despite that struvite ($MgNH_4PO_4$) was no detected by XRD analysis in loaded Ze-Mg1

10 samples, SEM images reported crystal structures and analysis of zeolite composition leads to

11 formulate that phosphate sorption mechanism is performed via the formation of magnesium

12 ammonium phosphate salts and probably, small quantities of calcium containing phosphate

13 minerals. Characterization of loaded Ze-Mg2 sample showed no changes compared to the virgin

14 zeolite structure and formation of magnesium aluminum silicate but struvite was not observed in

15 SEM images.

16 **Figure 4**

17

18 It is noteworthy that ammonium sorption was better described by the isotherm equations than for

19 phosphate. This is due to the fact that phosphate uptake is carried out mainly by formation of Ca

20 and Mg phosphate precipitation instead of ion exchange and processes involving chemical

21 reactions were not described by these theoretical models (e.g., formation of magnesium and

22 calcium phosphates and the mixed magnesium and ammonium phosphate).

23

24 **3.3 The influence of zeolite modification process on sorption mechanisms**

1 According to the removal patterns, the extraction of NH_4^+ ions by both Ze-Ca and Ze-Mg was

2 carried out mainly by ion exchange with Ca^{2+} and Mg^{2+} ions, respectively. The sorption

3 mechanism was verified by mass balance (Eq. 15) taking into account the adsorbed and released

4 ions with a deviation around 15% (data not shown). Furthermore, as is shown in Figure 5 and

5 was also confirmed by FSEM-EDS analysis of loaded zeolites reported a significant reduction of

6 zeolite cations exchanged (Ca/Mg) as a consequence of their release to the aqueous solution. It

7 is worth to mention that in the case of Ze-Mg1 and Ze-Mg2 the ion exchange is carried out not

8 only with magnesium ions but also with remaining sodium ions not exchanged during zeolite

9 modification process.

$$\Delta\,(\%) = \left| \frac{\frac{A}{d} - \frac{D}{a}}{A} \cdot 100 \right| \qquad\qquad \text{Eq. 15}$$

10 were A and D are the quantity of adsorbed and desorbed ions (mol), respectively, and a and d

11 are the absolute value of the ion charge of adsorbed and desorbed ions, respectively.

12 **Figure 5**

13 In the Figure 6 are shown the sorption capacity of Ze-Mg1 and Ze-Mg2 in both ammonium single

14 and ammonium/phosphate binary system.

15 **Figure 6**

16

17 Ze-Mg1 reported more than 100% higher ammonium sorption capacity than Ze-Mg2 in single

18 sorption experiments. A reduction of ammonium sorption capacity was observed only for Ze-Mg1

19 zeolites in the binary system, this trend is associated to the phosphate ions competence to form

20 ammonium-amino-phosphate salts. The high sodium content in Ze-Mg2 can explain this behavior,

21 whereas Ze-Mg1 is magnesium rich zeolite according to the values reported in Table 1. In

22 zeolites with high Silica Alumina Molar Rate (SAR), as in the case of zeolites used in this study, is

23 difficult to achieve complete ion exchange of divalent (in solution) by monovalent ions (in zeolite)

24 and this behavior is accentuated as smaller is the atomic radius of the divalent ion [8].

12

1   In the case of the binary system, ammonium and phosphate sorption capacity onto Ze-Mg2 was

2   lower approximately 40% and 60%, respectively compared to Ze-Mg1. This behavior is due to the

3   high quantity of sodium in the zeolite structure, not exchanged during the modification, as was

4   discussed in section 3.1.

5   In the case of the binary system, ammonium and phosphate sorption capacity onto Ze-Mg2 was

6   lower approximately 40% and 60%, respectively compared to Ze-Mg1. This behavior is due to the

7   high quantity of sodium in the zeolite structure, not exchanged during the modification, as was

8   discussed in section 3.1.

9   On one hand, it favors the competing ion effect between magnesium in the zeolite phase and

10   ammonium ions present in solution and on the other hand, it inhibits the precipitation of

11   phosphate minerals. Thus, the predominant sorption mechanism is ammonium ion exchange with

12   Na^+ cations instead of precipitation (struvite) as in the case of Ze-Mg1. Furthermore, in binary

13   system, Ze-Mg2 reported significantly lower sorption capacity for phosphate since ion exchange

14   is the main sorption mechanism instead the ammonium-phosphate-magnesium salts

15   precipitation.

16   The kinetic experiments were carried out only with Ze-Mg1 due to better sorption performance

17   reported compared to Ze-Mg2.

18   Is important to point out that in most of reviewed publications, both natural and modified zeolites

19   were used for either ammonium or phosphate removal from wastewater effluents, but few studies

20   have focused on evaluating the simultaneous phosphate and ammonium recovery. A comparison

21   of ammonium and phosphate sorption capacities reported for zeolitic sorbents is listed in Table 3.

22   The values reported in literature indicate that some differences can be observed depending on

23   the type of zeolite (natural or synthetic) and also in the form of the zeolite. It is worth to mention

24   that data is reported usually according to the Langmuir sorption capacity for that reason the

25   values reported in Table 3 are those obtained by this isotherm for different types of zeolites

13

1   (natural and synthetic). It can be observed a huge variability in sorption capacities from few mg/g

2   to 89 mg/g, which is the value, reported in this study for Ze-Ca. In the case of magnesium zeolite

3   the values are lower than calcium zeolite but are higher compared to those reported in literature.

4   Differences should be understood due to the different nature of the zeolites (natural and synthetic

5   or modified). The variation range with one order of magnitude from low values around 4 up to 90

6   mg/g is an indication of potential capacity of such materials. Then for practical concerns in full

7   scale applications it should be indicated that from the more conservative values expected (e.g., 4

8   to 20 mg/g) especially for natural zeolites the use of synthetic/and or modified of zeolites could

9   improve this capacity by a factor from 2 to 5.

10   **Table 3**

11

12 **3.4 Ammonium and phosphate sorption kinetics**

13 Kinetic data of ammonium and phosphate uptake by Ze-Ca and Ze-Mg1 are shown in Figure 7.

14 Both zeolites exhibited very fast kinetics as less than 20-30 minutes were necessary to reach the

15 equilibrium (fractional attainment of equilibrium >95%). However, ammonium showed faster

16 sorption rate than phosphate due to the ion exchange process is faster than the precipitation of

17 calcium and magnesium phosphate minerals.

18 It can be seen that in binary system, the uptake of both nutrients occurred at a fast rate during the

19 initial 15 minutes (fractional attainment of equilibrium >95%), followed by a slower process until

20 equilibrium is reached. This behavior was also observed in the use of zeolites for the uptake of

21 cephalexin [45], heavy metals [46,47], a cationic dye [48] or phenol [49].

22 Ze-Mg1 reported slightly higher sorption kinetic rate than Ze-Ca. Up to 80% of ammonium uptake

23 was reached before the first minute while Ze-Ca reported 50% of removal at the same time. This

24 behavior is due to the high SAR of both Ze-Ca and Ze-Mg1, which provides high selectivity for

25 monovalent ions and, the selectivity increases by increasing the size of the divalent ion, thus

14

1 zeolites showed higher affinity towards calcium ions which resulted in slower ammonium ion

2 exchange rate [8].

3 **Figure 7**

4 Kinetic experimental data were fitted to Eq. 6 – 10 and diffusion coefficients, the intraparticle

5 diffusion rate constants and the linear regression analyses are summarized in Table 4. HPDM

6 and SPM analysis showed that the particle diffusion was the rate-limiting step for both zeolites.

7 The sorption occurred mainly at the zeolite surface as dissolved nutrients may diffuse into zeolite

8 pores for interacting with the exchangeable cation.

9 The intraparticle diffusion model fitted well the experimental data and exhibit multi-linear plots

10 (Supplementary Material Fig. S2) indicating that the sorption process is performed in two steps.

11 Similar results were reported in studies performed with natural zeolites [11] and synthetic zeolites in

12 the adsorption of several pollutants such as ammonium, orthophosphate or heavy metals [50–53].

13 **Table 4**

14

15 As can be observed in Table 4, ammonium sorption in single and binary systems reported similar

16 particle diffusion coefficients for Ze-Ca, whereas Ze-Mg1 for binary kinetic experiments exhibited

17 higher values due to the precipitation of ammonium phosphate minerals, which reduces the

18 ammonium concentration on zeolite surface and favors the diffusion of ammonium ions from

19 aqueous solution. This trend can be corroborated by observing the concentration evolution of

20 ammonium in kinetic experiments of Ze-Mg1 (Figure 7), the ammonium sorption kinetics is faster

21 in ammonium phosphate binary system.

22 Moreover, in binary systems, phosphate sorption reported lower diffusion coefficients than

23 ammonium uptake for all sorbents as phosphate is negatively charged species and showed more

24 difficulties for being diffused into zeolite pores. This behavior can be also observed in Figure 7 as

25 phosphate concentration exhibited slower evolution in comparison with ammonium. Similar

15

1   results have been reported by Hermassi et al., when studying the extraction of phosphate by fly-

2   ash and synthetic zeolites in the calcium form [54-56].

3   The phosphate sorption process can be divided into two steps:

4   i) a first faster step consisted on Ca^{2+}/Mg^{2+} fast exchange with other ions present in solution (e.g.,

5   NH_4^+, Na^+) Eq. 16.

6   For Ze-Ca/Mg: $(-ZO^-)_2M^{2+} + 2\,N^+ \leftrightarrow 2\,(-ZO^-N^+) + M^{2+}$ fastest step   Eq. 16
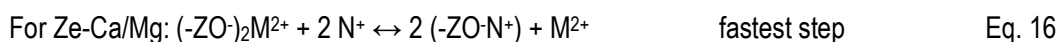
7   ii) and a second (slower) step where the phosphate ions once reached the boundary layer

8   interact with dissolved Ca(II) or Mg(II) as described by Eq. 17-18,

9   For Ze-Ca: $Ca^{2+} + HPO_4^{2-} \leftrightarrow CaHPO_4(s)$ slowest sorption step   Eq. 17

10   For Ze-Mg: $Mg^{2+} + HPO_4^{2-} + NH_4^+ \leftrightarrow MgNH_4PO_4(s) + H^+$ slowest sorption step   Eq. 18

11   Two-boundary reaction layers are formed in this two-step sorption process, i) the exchanged

12   Na^+/NH_4^+ layer and ii) the calcium phosphate and magnesium ammonium phosphate. The

13   combination of both steps is traduced in an integrated diffusion resistance, which results in higher

14   reaction times to reach equilibrium. Similar results have been reported by Guaya et al., using

15   natural zeolites impregnated with metal hydrated oxides on phosphate removal [57-58].

16

4. Conclusions

18   Activation of NaP1 zeolite to calcium and magnesium forms performed on sodium zeolitic

19   material synthesized from fly ash improved the zeolite phosphate sorption capacity in binary

20   systems while ammonium sorption capacity was reduced. The maximum sorption capacity

21   obtained for Ze-Ca was 123.1 ± 9.1 mg NH_4/g and 119.5 ± 7.5 mg PO_4/g in ammonium/phosphate

22   binary system.

23   The modification pre-treatment is temperature dependent as high SAR zeolites are more

24   selective to monovalent ions than divalent ions. Thus, increasing temperature during modification

25   step provides the energy required to exchange divalent ions by sodium ions in sodium zeolite.

26   This behavior was observed in the modification of zeolites to magnesium form, where high

16

1 temperature zeolite modification (Ze-Mg1) sorbent reported more than double magnesium

2 content than sorbent modified at room temperature (Ze-Mg2).

3 Phosphate sorption mechanism onto Ze-Ca is mainly due to the formation of phosphate minerals

4 such as calcium phosphate hydrated (brushite), which was confirmed by XRD analysis and in the

5 case of Ze-Mg it is due to the potential formation of struvite both on zeolite surface and into

6 aqueous solution.

7 The high affinity of Ca/Mg zeolites for ammonium and phosphate ions and the slow release of

8 ammonium and phosphate ions especially as they are removed through the formation of Ca- and

9 Mg-phosphates minerals, postulate these materials as potential carriers of nutrients for soil

10 quality improvement. Thus, the loaded zeolites, which contain ammonium and phosphate as well

11 as calcium or magnesium, could be potentially used as slow-release inorganic fertilizer.

12

13 **5. Acknowledgments**

19

20 **References**

21 1.   Water Environment Federation. Nutrient Removal. Fernandez R, Brown JA, Jones BG,
22   editors. Alexandria: McGraw Hill; 2010.

23 2.   Röhling S. Globale Verfügbarkeit von Dünger- und Energierohstoffen. In: AHT
24   Niederorschel und der Volksbank Dransfeld Proceedings. 2010.

25 3.   Groffman PM, Rosi-Marshall EJ. The Nitrogen Cycle. In: Weathers KC, Strayer DL, Likens
26   GE, editors. Fundamentals of Ecosystem Science. London: Elsevier; 2013. p. 212–45.

27 4.   Bennett EM, Schipanski ME. Chapter 8: The Phosphorus Cycle. In: Fundamental of
28   Ecosystem Science. Elsevier; 2013.

29 5.   Galloway J, Cowling E. Reactive nitrogen and the world: Two hundred yeards of change.

1. Ambio. 2002;31:64–71.

6. Driscoll CT, Whitall D, Aber J, Boyer E, Castro M, Cronan C, et al. Nitrogen pollution in the northeastern United States: Sources, effects and management options. Bioscience. 2003;53(4):357–74.

7. Tashauoei HR, Movahedian HA, Amin MM, Kamali M, Nikaeen M, Dastjerdi VM. Removal of cadmium and humic acid from aqueous solutions using surface modified nanozeolite A. Int J Environ Sci Technol. 2010;7(3):497–508.

8. Sherry HS. Ion Exchange. In: Auerbach SM, Carrado KA, Dutta PK, editors. Handbook of Zeolite Science and Technology. New York: Marcel Dekker, Inc.; 2003. p. 1006–61.

9. Ramesh K, Reddy DD, Biswas AK, Rao AS. Zeolites and Their Potential Uses in Agriculture. Adv Agron. 2011;113:215–36.

10. Sherry HS. Ion Exchange. In: Auerbach SM, Carrado KA, Dutta PK, editors. Handbook of Zeolite Science and Technology. New York: Marcel Dekker, Inc; 2003. p. 1006–61.

11. Guaya D, Valderrama C, Farran A, Armijos C, Cortina JL. Simultaneous phosphate and ammonium removal from aqueous solution by a hydrated aluminum oxide modified natural zeolite. Chem Eng J. 2015;271:204–13.

12. Schick J, Caullet P, Paillaud J-L, Patarin J, Freitag S, Mangold-Callarec C. Phosphate uptake from water on a Surfactant-Modified Zeolite and Ca-zeolites. J Porous Mater. 2011 Jul 15;19(4):405–14.

13. Alshameri A, Yan C, Al-Ani Y, Dawood AS, Ibrahim A, Zhou C, et al. An investigation into the adsorption removal of ammonium by salt activated Chinese (Hulaodu) natural zeolite: Kinetics, isotherms, and thermodynamics. J Taiwan Inst Chem Eng [Internet]. Taiwan Institute of Chemical Engineers; 2014;45(2):554–64. Available from: http://dx.doi.org/10.1016/j.jtice.2013.05.008

14. Alshameri A, Yan C, Lei X. Enhancement of phosphate removal from water by TiO2/Yemeni natural zeolite: Preparation, characterization and thermodynamic. Microporous Mesoporous Mater. 2014;196:145–57.

15. Wu D, Zhang B, Li C, Zhang Z, Kong H. Simultaneous removal of ammonium and phosphate by zeolite synthesized from fly ash as influenced by salt treatment. J Colloid Interface Sci. 2006 Dec 15;304(2):300–6.

16. Yang M, Lin J, Zhan Y, Zhang H. Adsorption of phosphate from water on lake sediments amended with zirconium-modified zeolites in batch mode. Ecol Eng. 2014;71:223–33.

17. Ramesh K, Biswas AK, Somasundaram J, Subba Rao A. Nanoporous zeolites in farming: Current status and issues ahead. Curr Sci. 2010;99(6):760–5.

18. Abdi GH, Khui MK, Eshghi S. Effects on natural zeolite on growth and flowering on strawberry. Int J Agric Res. 2006;1:384–9.

19. Gruener JE, Ming DW, Henderson KE, Galindo C. Common ion effects in zeoponic substrates: Wheat plant growth experiment. Microporous Mesoporous Mater. 2003;61:223–30.

20. McGilloway R, Weaver R, Ming D, Gruener JE. Nitrification in a zeoponic substrate. Plant Soil. 2003;256:371–8.

21. Hua QX, Zhou JM, Wang HY, Du CW, Chen XQ, Li JY. Effects of modified clinoptilolite on phosphorus mobilisation and potassium or ammonium release in Ferrosols. Aust J Soil Res. 2006;44:285–90.

22. Kim Y-S, Lee Y-H, An B, Choi S-A, Park J-H, Jurng J-S, et al. Simultaneous Removal of Phosphate and Nitrate in Wastewater Using High-Capacity Anion-Exchange Resin. Water, Air, Soil Pollut. 2012 Sep 22;223(9):5959–66.

23. Takaya CA, Fletcher LA, Singh S, Anyikude KU, Ross AB. Phosphate and ammonium sorption capacity of biochar and hydrochar from different wastes. Chemosphere. Elsevier Ltd; 2016;145:518–27.

24. Bassin JP, Kleerebezem R, Dezotti M, van Loosdrecht MCM. Simultaneous nitrogen and phosphate removal in aerobic granular sludge reactors operated at different temperatures. Water Res. 2012 Aug;46(12):3805–16.

25. Marcelino M, Wallaert D, Guisasola A, Baeza J a. A two-sludge system for simultaneous biological C, N and P removal via the nitrite pathway. Water Sci Technol. 2011 Sep;64(5):1142.

26. Zhang B-H, Wu D-Y, Wang C, He S-B, Zhang Z-J, Kong H-N. Simultaneous removal of ammonium and phosphate by zeolite synthesized from coal fly ash as influenced by acid treatment. J Environ Sci (China). 2007 Jan;19(5):540–5.

27. Querol X, Moreno N, Alastuey a, Juan R, Ayora C, Medinaceli A. Synthesis of high ion exchange zeolites from coal fly ash. Geol Acta. 1996;1:49–57.

28. Moreno N, Querol X, Ayora C, Pereira CF, Janssen-Jurkovicová M. Utilization of zeolites synthesized from coal fly ash for the purification of acid mine waters. Environ Sci Technol. 2001;35(17):3526–34.

29. You X, Guaya D, Farran A, Valderrama C, Cortina JL. Phosphate removal from aqueous solution using a hybrid impregnated polymeric sorbent containing hydrated ferric oxide (HFO). J Chem Technol Biotechnol [Internet]. 2015 Jan 2 [cited 2015 Mar 17]; Available from: http://doi.wiley.com/10.1002/jctb.4629

30. Liberti L, Passino R. Chapter 3. In: Marinsky JA, Marcus Y, editors. Ion Exchange and Solvent Extraction, vol 7. New York: Marcel Dekker, Inc.; 1977.

31. Helfferich F. Ion Exchange. New York: Mc Graw Hill; 1962.

32. Valderrama C, Barios JI, Caetano M, Farran A, Cortina JL. Kinetic evaluation of phenol/aniline mixtures adsorption from aqueous solutions onto activated carbon and hypercrosslinked polymeric resin (MN200). React Funct Polym. 2010 Mar;70(3):142–50.

33. Lin L, Lei Z, Wang L, Liu X, Zhang Y, Wan C, et al. Adsorption mechanisms of high-levels of ammonium onto natural and NaCl-modified zeolites. Sep Purif Technol. 2013;103:15–20.

34. Xie J, Meng W, Wu D, Zhang Z, Kong H. Removal of organic pollutants by surfactant modified zeolite: Comparison between ionizable phenolic compounds and non-ionizable organic compounds. J Hazard Mater [Internet]. Elsevier B.V.; 2012;231-232:57–63. Available from: http://dx.doi.org/10.1016/j.jhazmat.2012.06.035

35. Li J, Qiu J, Sun Y, Long Y. Studies on natural STI zeolite: modification, structure, adsorption and catalysis. Microporous Mesoporous Mater. 2000;37:365–78.

36. Huang H, Xiao D, Pang R, Han C, Ding L. Simultaneous removal of nutrients from simulated swine wastewater by adsorption of modified zeolite combined with struvite crystallization. Chem Eng J. 2014;256:431–8.

37. Xie J, Li C, Chi L, Wu D. Chitosan modified zeolite as a versatile adsorbent for the removal of different pollutants from water. Fuel. 2013 Jan;103:480–5.

38. Englert a. H, Rubio J. Characterization and environmental application of a Chilean natural

19

zeolite. Int J Miner Process. 2005;75(1-2):21–9.

39. Huang H, Xiao X, Yan B, Yang L. Ammonium removal from aqueous solutions by using natural Chinese (Chende) zeolite as adsorbent. J Hazard Mater. 2010;175(1-3):247–52.

40. Zhang M, Zhang H, Xu D, Han L, Niu D, Zhang L, et al. Ammonium removal from aqueous solution by zeolites synthesized from low-calcium and high-calcium fly ashes. Desalination. 2011;277(1-3):46–53.

41. Wang YF, Lin F, Pang WQ. Ammonium exchange in aqueous solution using Chinese natural clinoptilolite and modified zeolite. J Hazard Mater. 2007;142(1-2):160–4.

42. Zheng H, Han L, Ma H, Zheng Y, Zhang H, Liu D, et al. Adsorption characteristics of ammonium ion by zeolite 13X. J Hazard Mater. 2008;158(2-3):577–84.

43. Zhao Y, Zhang B, Zhang X, Wang J, Liu J, Chen R. Preparation of highly ordered cubic NaA zeolite from halloysite mineral for adsorption of ammonium ions. J Hazardous Mater. 2010; 178:658–664.

44. Khosravi A, Esmhosseini M, Khezri S. Removal of ammonium ion from aqueous solutions using natural zeolite: kinetic, equilibrium and thermodynamic studies. Res Chem Intermed. 2014; 40:2905–2917

45. Samarghandi MR, Al-Musawi TJ, Mohseni-Bandpi A, Zarrabi M. Adsorption of cephalexin from aqueous solution using natural zeolite and zeolite coated with manganese oxide nanoparticles. J Mol Liq. 2015;211:431–41.

46. Javadian H, Ghorbani F, Tayebi H, Asl SMH. Study of the adsorption of Cd (II) from aqueous solution using zeolite-based geopolymer, synthesized from coal fly ash; kinetic, isotherm and thermodynamic studies. Arab J Chem. 2015;8:837–49.

47. Pandey PK, Sharma SK, Sambi SS. Removal of lead(II) from waste water on zeolite-NaX. J Environ Chem Eng. 2015;3:2604–10.

48. Panic V V., Velickovic SJ. Removal of model cationic dye by adsorption onto poly(methacrylic acid)/zeolite hydrogel composites: Kinetics, equilibrium study and image analysis. Sep Purif Technol. 2014;122:384–94.

49. Yousef RI, El-Eswed B, Al-Muhtaseb AH. Adsorption characteristics of natural zeolites as solid adsorbents for phenol removal from aqueous solutions: Kinetics, mechanism, and thermodynamics studies. Chem Eng J. Elsevier B.V.; 2011 Jul;171(3):1143–9.

50. Jovanovic M, Grbavcic Z, Rajic N, Obradovic B. Removal of Cu(II) from aqueous solutions by using fluidized zeolite A beads: Hydrodynamic and sorption studies. Chem Eng Sci. 2014;117:85–92.

51. Kong X, Han Z, Zheng W, Song L, Li H. Synthesis of zeolite-supported microscale zero-valent iron for the removal of Cr6+ and Cd2+ from aqueous solution. J Environ Manage. 2016;169:84–90.

52. Huang H, Yang L, Xue Q, Liu J, Hou L, Ding L. Removal of ammonium from swine wastewater by zeolite combined with chlorination for regeneration. J Environ Manage. 2015;160:333–41.

53. Lin L, Wan C, Lee D, Lei Z, Liu X. Ammonium assists orthophosphate removal from high-strength wastewaters by natural zeolite. Sep Purif Technol [Internet]. Elsevier B.V.; 2014;133:351–6. Available from: http://dx.doi.org/10.1016/j.seppur.2014.07.010

54 Hermassi, M., Valderrama, C., Moreno, N., Font, O., Querol, X., Batis, N.H., Cortina, J.L.Fly ash as reactive sorbent for phosphate removal from treated waste water as a potential slow release fertilizer (2017) Journal of Environmental Chemical Engineering, 5

20

1 (1), 160-169.

2 55 Hermassi, M., Valderrama, C., Moreno, N., Font, O., Querol, X., Batis, N., Cortina, J.L.
3 Powdered Ca-activated zeolite for phosphate removal from treated waste-water (2016)
4 Journal of Chemical Technology and Biotechnology, 91 (7), 1962-1971.

5 56 Hermassi, M., Valderrama, C., Gibert, O., Moreno, N., Font, O., Querol, X., Batis, N.H.,
6 Cortina, J.L. Integration of Powdered Ca-Activated Zeolites in a Hybrid Sorption-
7 Membrane Ultrafiltration Process for Phosphate Recovery (2016) Industrial and
8 Engineering Chemistry Research, 55 (21), 6204-6212.

9 57 Guaya, D., Hermassi, M., Valderrama, C., Farran, A., Cortina, J.L., Recovery of
10 ammonium and phosphate from treated urban wastewater by using potassium
11 clinoptilolite impregnated hydrated metal oxides as N-P-K fertilizer (2016) Journal of
12 Environmental Chemical Engineering, 4 (3), pp. 3519-3526.

13 58 Guaya, D., Valderrama, C., Farran, A., Cortina, J.L., Modification of a natural zeolite with
14 Fe(III) for simultaneous phosphate and ammonium removal from aqueous solutions
15 (2016) Journal of Chemical Technology and Biotechnology, 91 (6), pp. 1737-1746.

1   Table 1. Chemical composition (wt %) of raw Ze-Na and salt modified zeolites Ze-Ca, Ze-Mg1

2   and Ze-Mg2.

Element	Ze-Na	Ze-Ca	Ze-Mg1	Ze-Mg2
O	55.7	57.6	58.8	59.3
Na	9.1	0.3	2.2	5.7
Mg	0.8	0.8	4.3	1.9
Al	10.4	9.6	10.3	10.1
Si	19.4	19.0	17.8	18.8
Ca	1.6	9.4	1.0	1.6
Fe	2.9	3.3	5.5	2.6

3

4

1   Table 2. Langmuir, Freundlich and Langmuir-Freundlich isotherm parameters for ammonium

2   removal onto Ze-Ca, Ze-Mg1 and Ze-Mg2.

3

		Langmuir			Freundlich			Langmuir-Freundlich			
		ARE (%)	K_L	q_m	ARE (%)	K_F	n	ARE (%)	q_m	K_{LF}	N
Ze-Ca	Ammonium single	20	$(2\pm 0.4) \times 10^{-3}$	93±19	17	1.44±0.2	1.85	14	135±19	$(1.2 \pm 0.17) \times 10^{-4}$	0.7
	Binary Ammonium	22	$(3\pm 0.7) \times 10^{-3}$	89±20	12	2.49±0.3	2.20	7	123±9	7.4×10^{-4}	0.6
	Binary Phosphate	7	$(3\pm 0.2) \times 10^{-3}$	115±8	25	1.81±0.5	2.03	6	120±7	$(2\pm 0.1) \times 10^{-3}$	1
Ze-Mg1	Ammonium single	31	$(1.3\pm 0.4) \times 10^{-2}$	49±15	15	5.04±0.8	3.00	10	89±9	$(1\pm 0.1) \times 10^{-3}$	0.4
	Binary Ammonium	24	0.125±0.03	25±6	6	4.64±0.3	3.72	4	55±2	$(2\pm 0.1) \times 10^{-3}$	0.4
	Binary Phosphate	27	$(3.8\pm1) \times 10^{-4}$	35±9	55	0.32±0.18	2.83	24	60±14	$(1.1\pm0.26) \times 10^{-4}$	0.9
Ze-Mg2	Ammonium single	8	$(8\pm 0.6) \times 10^{-3}$	58±5	29	1.45±0.4	2.13	11	31±3	$(2.2\pm 0.2) \times 10^{-2}$	1.2
	Binary Ammonium	9	$(3.7\pm 0.3) \times 10^{-2}$	24±2	15	3.31±0.5	3.34	6	32±2	$(1.2\pm 0.07) \times 10^{-2}$	0.7
	Binary Phosphate	27	$(4\pm 1.1) \times 10^{-3}$	9±2	20.5	0.91±0.2	3.51	19	24±4	$(8.9\pm1.7) \times 10^{-5}$	0.4

4

23

1

2   Table 3. Ammonium and phosphate sorption capacities obtained in this study and comparison

3   with data reported in literature for different zeolitic sorbents.

Zeolite	Zeolitic form	Recovered nutrient	Sorption capacity [mg/g]	Reference
Ze-Ca	Ca^{2+}	NH_4^+	89±20	This study
		PO_4^{3-}	115±8	
Ze-Mg1	Mg^{2+}	NH_4^+	25±6	
		PO_4^{3-}	35±9	
Ze-Mg2	Mg^{2+}, Na^+	NH_4^+	24±2	
		PO_4^{3-}	9±2	
CMZFA	$-NH_2$	PO_4^{3-}	4.1	[37]
Ch-zeolite	Na^+, K^+	NH_4^+	10.6	[38]
ActZ (NaCl)	Na^+	NH_4^+	5.9	[13]
ActZ (NaOH)	Na^+	NH_4^+	4.6	
Chende-Ze	Na^+	NH_4^+	9.4	[39]
LC-Z	Ca^{2+}	NH_4^+	28.7	[40]
HC-Z	Ca^{2+}	NH_4^+	6.1	
Na-Y	Na^+	NH_4^+	22.6	[41]
13X	K^+	NH_4^+	8.6	[42]
NaA zeolite	Na^+	NH_4^+	44.3	[43]
Acid treat. zeolite (Azerbaijan)	Na^+	NH_4^+	43.7	[44]

4

5

1

2

3

4

5

6

7

8

9

10

11

12

13

14

15

16

17

18

19

20

21

22

23

24

25

26

27

28

29

30

31

32

33

34

35

36

37

38

39

40

41

42

43

44

45

46

47

48

49

50

51

52

53

54

55

56

57

58

59

60

1   Table 4. Kinetic parameters obtained by HPDM, SPM and intraparticle diffusion model for ammonium and

2   phosphate uptake by Ze-Ca and Ze-Mg1

		HPDM				SPM					
		Fluid film		Particle diffusion		Fluid film		Particle diffusion		Chemical reaction	
		D	R^2	D_e	R^2	K_F	R^2	D_e	R^2	K_s	R^2
Ze-Ca											
NH_4^+ Single		$(7.04\pm0.35)\times10^{-9}$	0.95	$(3.6\pm0.07)\times10^{-14}$	0.98	$(8.6\pm1.5)\times10^{-10}$	0.82	$(3.4\pm0.17)\times10^{-14}$	0.95	$(3.6\pm0.25)\times10^{-10}$	0.93
NH_4^+/PO	NH_4^+	$(8.9\pm0.16)\times10^{-9}$	0.98	$(5.3\pm0.05)\times10^{-14}$	0.99	$(6.4\pm4.5)\times10^{-10}$	0.27	$(5.1\pm0.15)\times10^{-14}$	0.97	$(4.7\pm0.19)\times10^{-10}$	0.96
4^{3-} binary	PO_4^{3-}	$(3.6\pm0.36)\times10^{-9}$	0.90	$(2.0\pm0.14)\times10^{-14}$	0.93	$(8.5\pm1.7)\times10^{-10}$	0.80	$(2.1\pm0.21)\times10^{-14}$	0.90	$(2.4\pm0.34)\times10^{-10}$	0.86
Ze-Mg1											
NH_4^+ Single		$(6.9\pm1.31)\times10^{-9}$	0.81	$(4.0\pm0.36)\times10^{-14}$	0.91	$(2.0\pm0.76)\times10^{-10}$	0.62	$(3.8\pm0.42)\times10^{-14}$	0.89	$(2.1\pm0.21)\times10^{-10}$	0.90
NH_4^+/PO	NH_4^+	$(1.1\pm0.06)\times10^{-8}$	0.95	$(7.3\pm0.07)\times10^{-13}$	0.99	$(2.6\pm0.47)\times10^{-10}$	0.82	$(6.7\pm0.13)\times10^{-13}$	0.98	$(2.9\pm0.29)\times10^{-10}$	0.90
4^{3-} binary	PO_4^{3-}	$(4.8\pm0.29)\times10^{-9}$	0.94	$(2.5\pm0.08)\times10^{-14}$	0.97	$(1.3\pm0.29)\times10^{-9}$	0.78	$(2.6\pm0.10)\times10^{-14}$	0.96	$(2.9\pm0.29)\times10^{-10}$	0.90

3

25

1
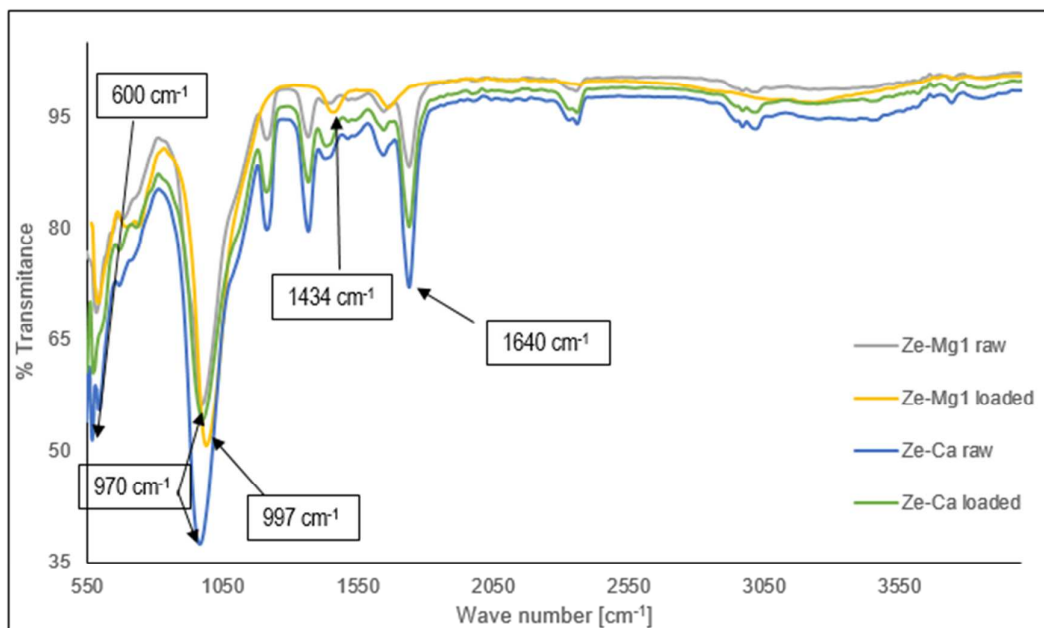
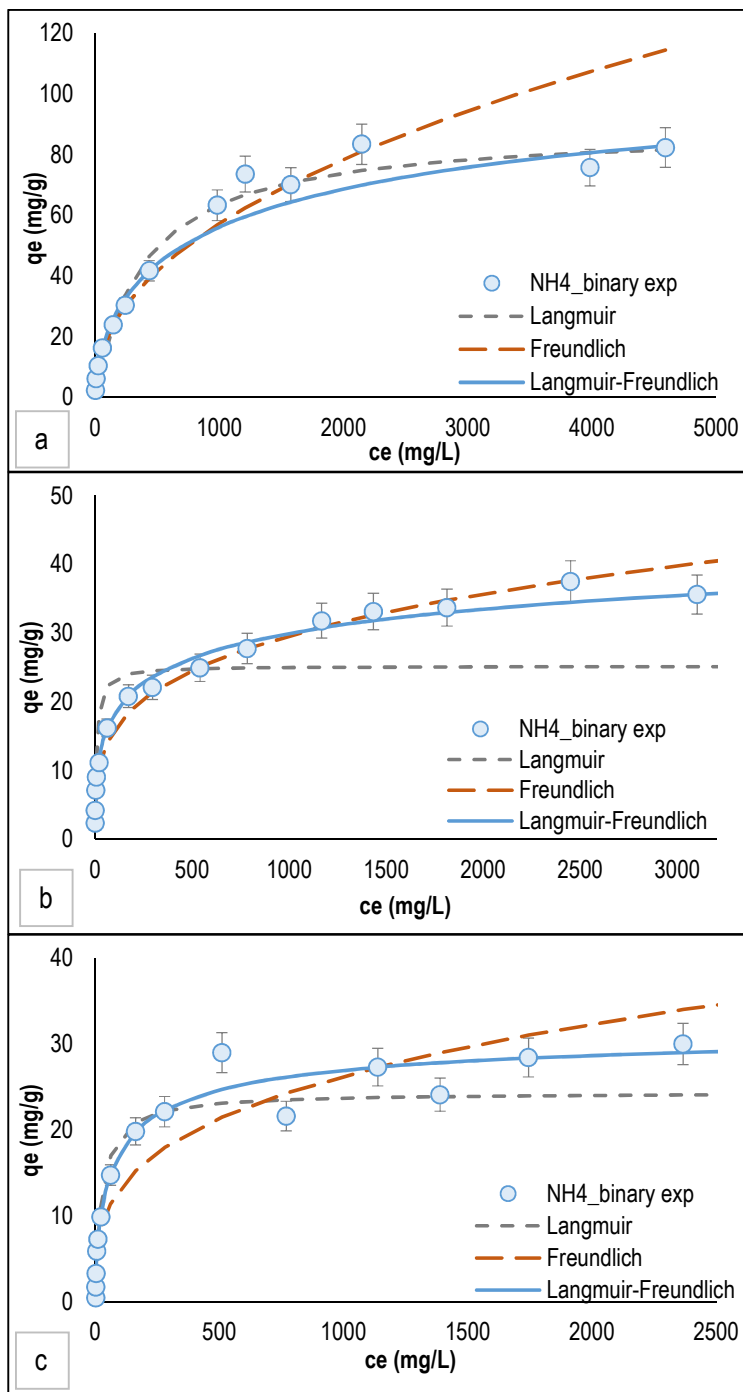Figure 1. FTIR spectroscopy of raw and loaded zeolites Ze-Ca and Ze-Mg1.

Figure 2. Experimental and theoretical equilibrium isotherm for ammonium removal in: a) Ze-Ca, b) Ze-Mg1 and c) Ze-Mg2.
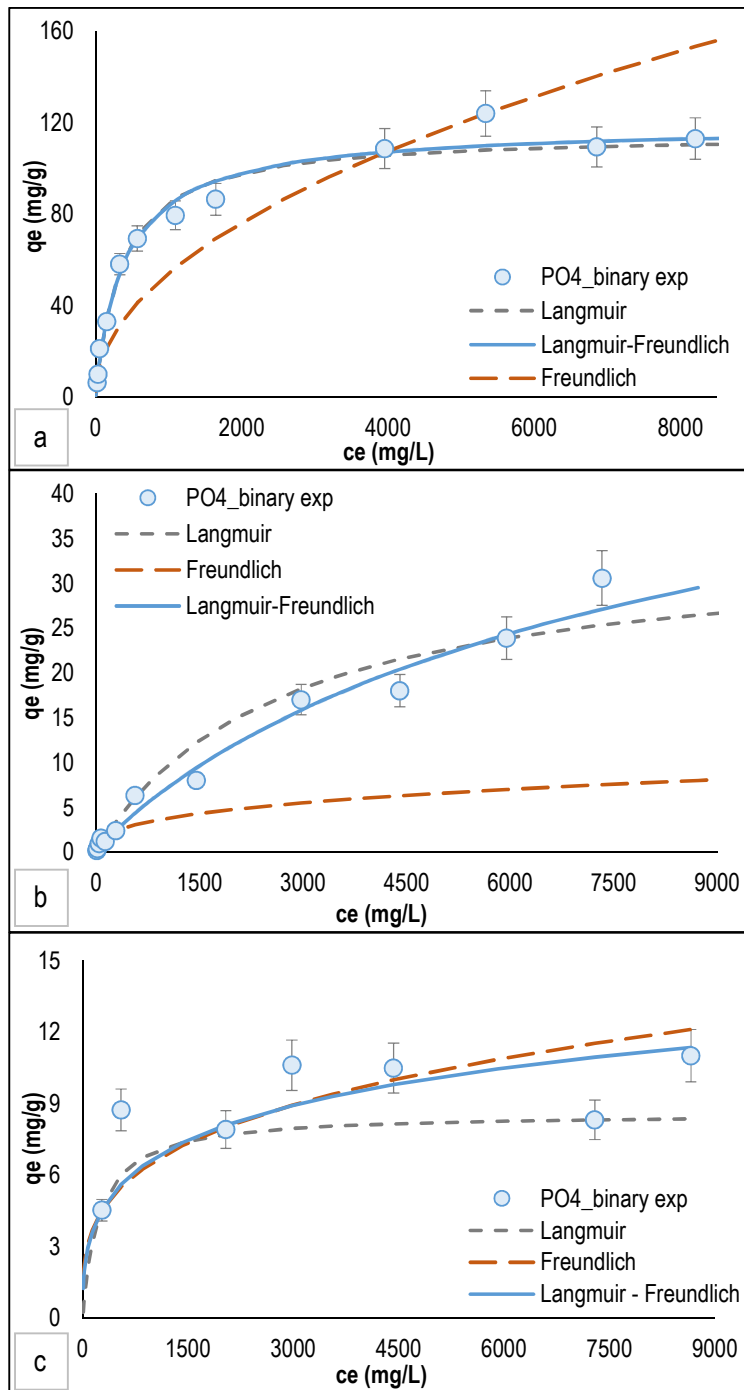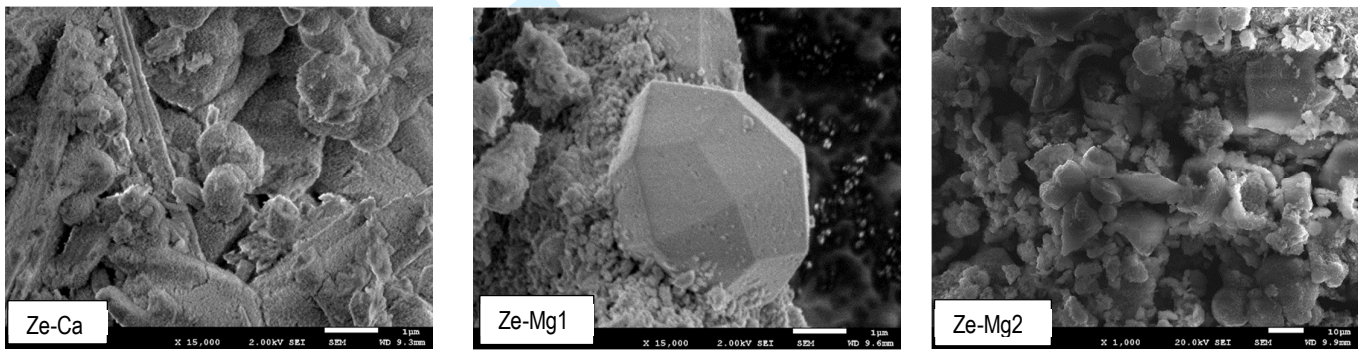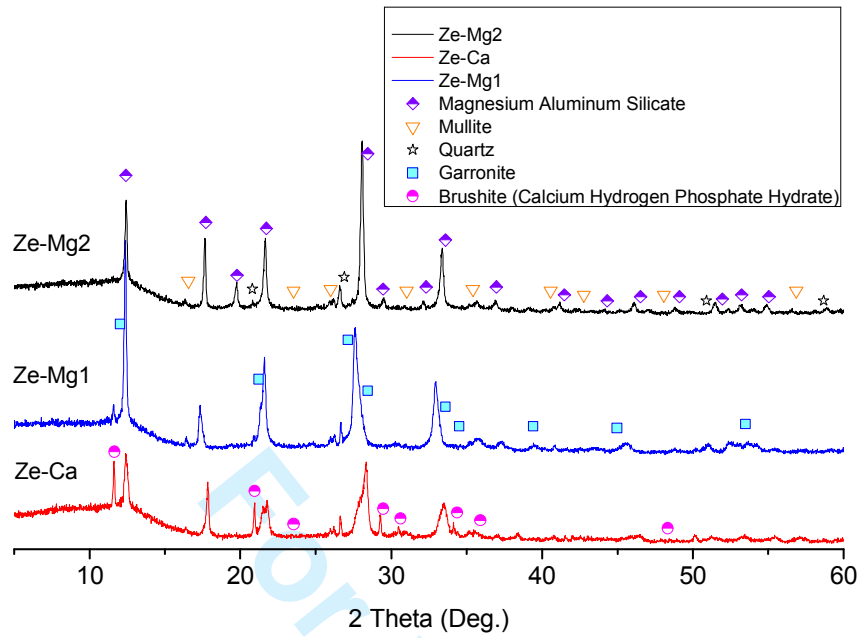
Figure 3. Experimental and theoretical equilibrium isotherm for phosphate removal in: a) Ze-Ca,

b) Ze-Mg1 and c) Ze-Mg2

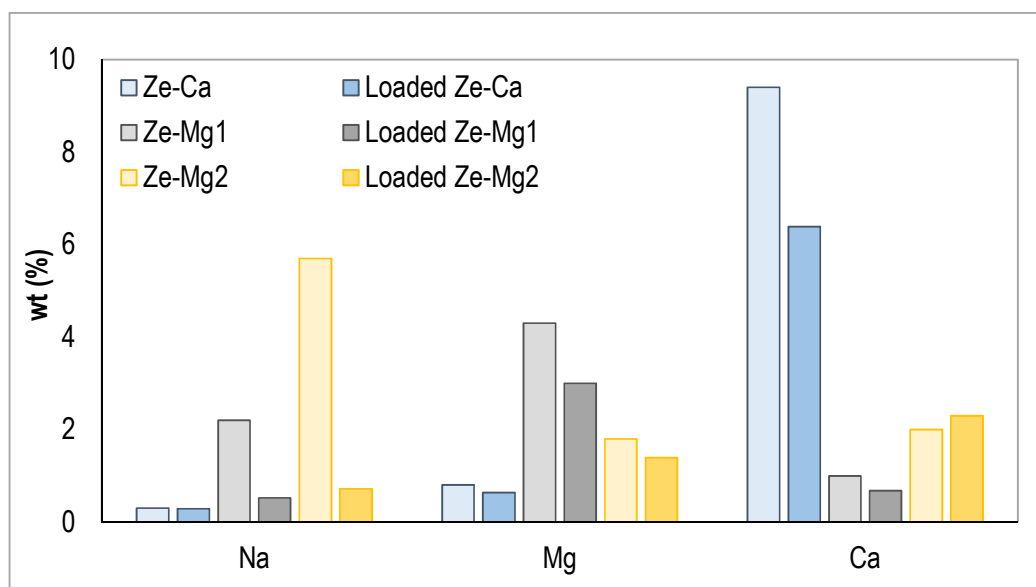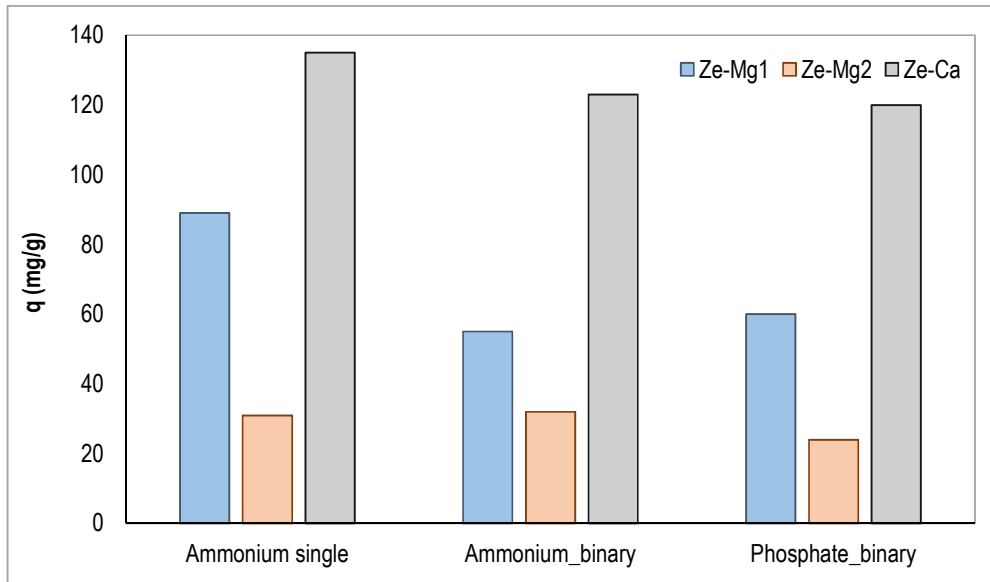Figure 4. XRD patterns and SEM images for loaded zeolites Ze-Ca, Ze-Mg1 and Ze-Mg2.

Figure 5. Mass content of ions exchanged in virgin and loaded zeolites.

Figure 6. Lagmuir-Freundlich Sorption capacity of ammonium single and ammonium/phosphate binary system onto Ze-Ca, Ze-Mg1 and Ze-Mg2.
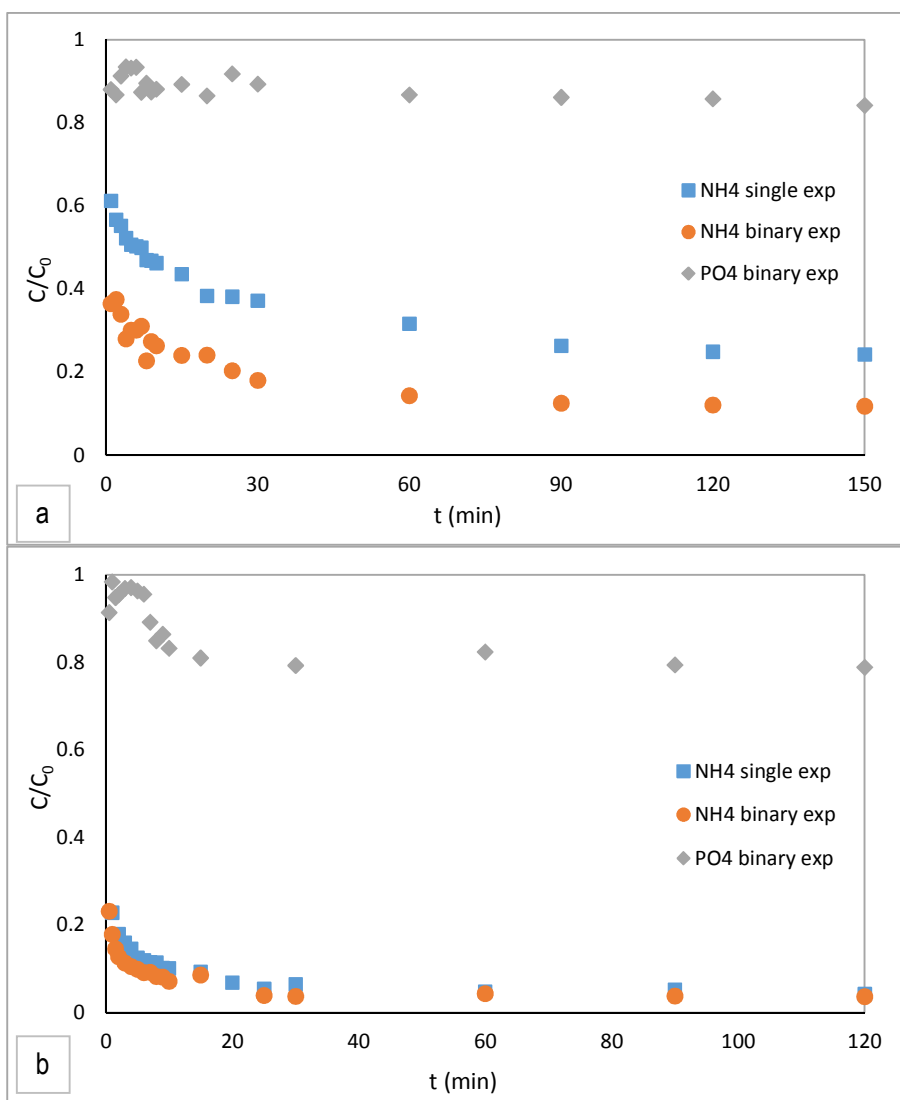
Figure 7. Evolution of ammonium and phosphate concentration as a function of time for a) Ze-Ca and b) Ze-Mg1.

Simultaneous recovery of ammonium and phosphate from simulated treated wastewater effluents by activated calcium and magnesium zeolites

Xialei You[a*], César Valderrama[a] and José Luis Cortina[a,b]

[a] Department of Chemical Engineering. Universitat Politècnica de Catalunya-Barcelona-TECH (UPC), Spain

[b] Water Technology Center, CETaqua, Carretera d'Esplugues 75, Cornellá de Llobregat, 08940 Spain

*Correspondence should be addressed to: Xialei You

Departament of Chemical Engineering, Universitat Politècnica de Catalunya-Barcelona Tech (UPC)

Avda. Diagonal, 647 (08028) Barcelona, Spain

Tel.: 93 401 66 45

Email: xialei.you@upc.edu
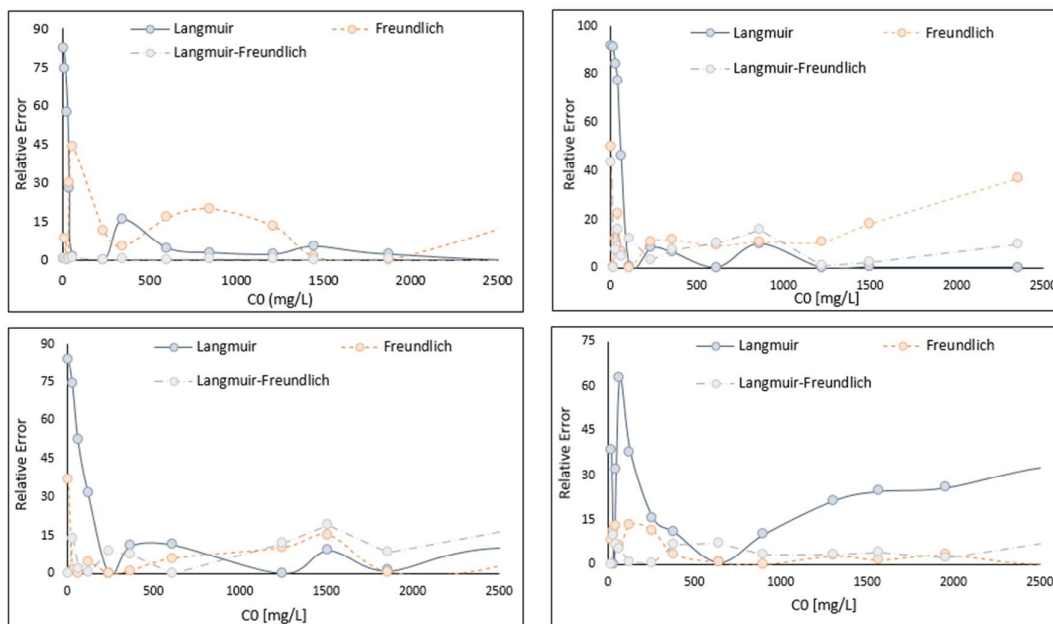
Supplementary Material

Figure S1. Relative Error for ammonium adsorption on Ze-Ca and Ze-Mg1 according to Langmuir, Freundlich and Langmuir-Freundlich isotherm model
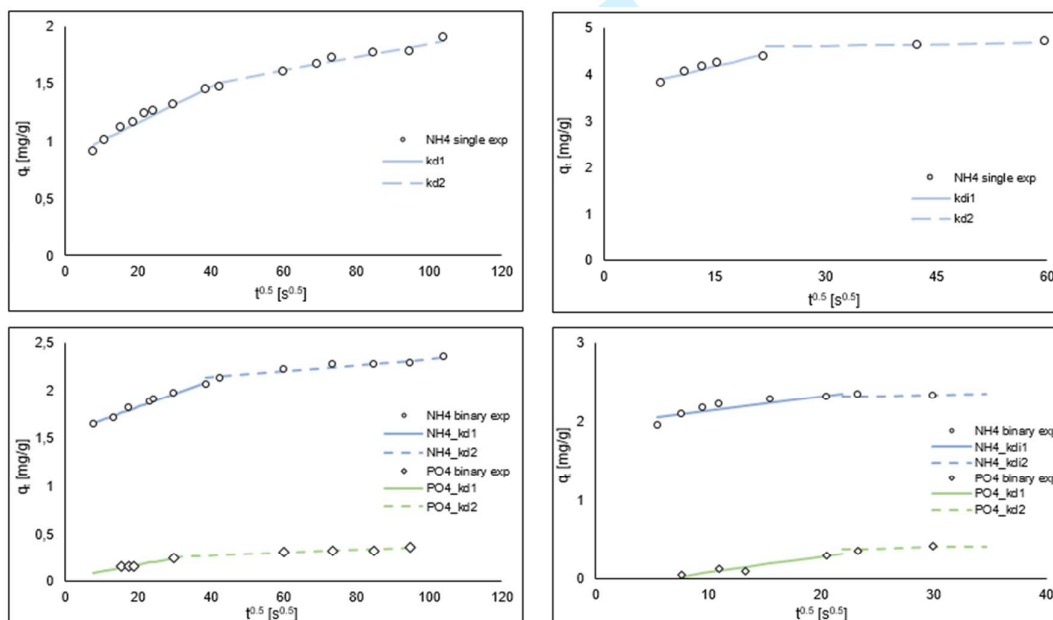

Figure S2. Intraparticle diffusion kinetics for ammonium and phosphate adsorption on a) Ze-Ca and b) Ze-Mg1 in single and binary system